2021

Performance Evaluation of Three Virtual Metering Methods to Estimate Zone-level Perimeter Heater Energy Requirement

Darwish Darwazeh
Carleton University, darwish.darwazeh@carleton.ca

Jean Duquette

Burak Gunay

Performance evaluation of three virtual metering methods to estimate zone-level perimeter heater energy requirement

Darwish Darwazeh[1,*], Jean Duquette[2], and Burak Gunay[1]

[1] Carleton University, Department of Civil and Environmental Engineering, Ottawa, Ontario, Canada
[2]Carleton University, Department of Mechanical and Aerospace Engineering, Ottawa, Ontario, Canada
* Corresponding author e-mail address: darwish.darwazeh@carleton.ca

ABSTRACT

Virtual metering provides a cost-effective alternative to physical meters to monitor building energy performance and capture unmetered energy flows at the zone-level. Virtual metering accuracy depends on the modelling method and its ability to represent the heating and cooling processes at a building thermal zone. This paper employs three virtual metering methods to estimate the heating energy of zone-level perimeter heaters: a steady-state modelling method, a transient modelling method, and a load disaggregation modelling method. Inverse models representing these three virtual metering methods are trained using data obtained from seven perimeter offices in an academic building in Ottawa, Canada. Model parameters are identified using the genetic algorithm and used for creating virtual meters that estimate the energy requirement of zone-level perimeter heaters. The virtual meters' accuracy is assessed by comparing the results to measured heating energy obtained from physical meters installed in the seven offices. The three virtual metering methods' performance is evaluated through illustrative examples in terms of modelling assumptions, data requirements, and virtual metering accuracy. The results indicate that the three virtual metering methods can estimate the daily heating energy supplied by perimeter heaters at a normalized root-mean-square error between 13% and 23%.

1. INTRODUCTION

Metering of building heating and cooling energy at the zone-level is uncommon due to cost and practical issues, leaving critical quantities unmeasured such as the heat added by perimeter radiant heaters. Virtual metering provides a non-intrusive alternative to physical meters that can capture zone-level unmetered energy flows by utilizing available sensor and actuator measurements from a building automation system (BAS). Virtual meters (VMs) can be employed at a building zone-level to support operational decisions and improve energy performance and occupant comfort by allowing early detection of operational inefficiencies. However, virtual metering accuracy depends on the modelling method utilized and its ability to represent zone-level heating and cooling processes. These modelling methods involve assumptions regarding data processing and the degree to which the model agrees with the physical reality.

Selection of a suitable modelling method that can represent energy flows at a building thermal zone is essential for developing accurate zone-level VMs, describing building energy performance, identifying energy consumption patterns, developing model-based predictive control strategies, and detecting zone-level system faults (Bacher & Madsen, 2011; Gunay et al., 2016). The process of developing a zone model includes the selection of a model structure, the estimation of model parameters, and model validation (Madsen et al., 2016). The purpose of the zone model and the measured data available from a building thermal zone guide selecting a suitable model structure. Data collected from zone-level sensors, meters, and actuators are processed and used to train the model. Model parameters that represent unmeasured values are estimated using a model optimization algorithm that fits the model prediction to measured values (Balan et al., 2011). These estimated model parameters should be within a reasonable range of the underlying physical characteristics they represent; for example, an over-estimated value for the parameter representing the zone thermal resistance under ideal operating conditions indicates an unsuitable model structure.

VMs can be used to estimate unmetered heating energy of zone-level heating devices to understand its impact on the energy consumption of a building. Perimeter zones are subjected to internal heat gains from lights, occupants, and equipment, solar heat gains through windows, and heat gains by transmission through the envelope. The zone air temperature setpoint is maintained using supply air provided by an air handling unit (AHU) through a variable air volume (VAV) terminal box. These zones are often equipped with hydronic radiant heaters to satisfy the heating loads.

VMs can be employed to estimate the heat added by hydronic radiant heaters using the following three distinct modelling methods that emulate the heat transfer mechanisms within a given perimeter zone:

(1) *A steady-state inverse greybox modelling method*: this modelling method is useful for describing linear and stationary relations between model inputs and output (Madsen, 2008; Madsen et al., 2016) by assuming no energy is stored within the zone (Nassif et al., 2008a). The measurements' sampling time is usually averaged over a longer period since the system's dynamic behaviour is not described (Madsen et al., 2016; Rabl, 1988). Steady-state models are commonly used to evaluate energy efficiency measures and retrofit performance (Corrado & Fabrizio, 2007; Dall' o' et al., 2012; Firth & Lomas, 2009; Heo et al., 2012), and to find the effective thermal resistance of a building wall (Albatici et al., 2015; Nardi et al., 2015; Zheng, Cho et al., 2016).
(2) *A transient inverse greybox modelling method*: this modelling method describes the dynamic behaviour of the zone at different levels of complexity (Afram & Janabi-Sharifi, 2014b; Rabl, 1988). Heat transfer mechanisms are usually approximated by an equivalent thermal resistance-capacitance network (*i.e.*, RC network) (Gunay et al., 2017; Madsen et al., 2016). Transient models are typically used to evaluate building retrofits (Abushakra, 1999; Braun & Chaturvedi, 2002; Dong et al., 2005), to develop model-based predictive control strategies (Candanedo et al., 2013; Gunay et al., 2014; Ma et al., 2012; Široký et al., 2011), to detect HVAC system faults (Capozzoli et al., 2015; Ranade et al., 2020; Shi et al., 2016), and to characterize heating and cooling load patterns (Gunay et al., 2017; Wang et al., 2016).
(3) *A load disaggregation modelling method*: this modelling method breaks down the total load measured at the source into subsystem loads. The disaggregated loads provide a better understanding of the subsystems' energy performance (Yan et al., 2012). Load disaggregation models are commonly used in the literature to disaggregate the total electricity load across zone-level appliances in buildings (Dinesh et al., 2016; Patri et al., 2014; Valovage & Gini, 2017), and to disaggregate building total water consumption across zone-level water devices (Larson et al., 2012; Wang et al., 2018).

While models derived from these modelling methods are proposed in the literature for building energy management and building operation applications, to our knowledge, no comparisons have been made of these three modelling methods for virtual metering of heat added by perimeter radiant heaters. To this end, this paper analyzes the performance of the three modelling methods by developing VMs to estimate the heat added by zone-level perimeter heaters. Data obtained from seven perimeter offices in a highly instrumented academic building in Ottawa, Canada, are used to train the models. The accuracy of the VMs is assessed by comparing the results to measured heat obtained from physical meters installed in these seven offices. The modelling methods' performance is demonstrated through illustrative examples that compare modelling assumptions, data requirements, and virtual metering accuracy.

2. METHODOLOGY

As illustrated in Fig. 1, three distinct zone model structures are formulated via the application of a steady-state inverse greybox modelling method, a transient inverse greybox modelling method, and a load disaggregation modelling method. Data obtained from seven perimeter offices are used to train the models. Model parameters are identified using the genetic algorithm (GA) and used to develop VMs to estimate the heating energy of zone-level radiant heaters. VM results are compared with measured heat data obtained from physical meters installed at Zones (1) to (7). The root-mean-square error normalized by the range of daily measured heat at each radiant heater (NRMSE) is used to verify the accuracy of the VMs and evaluate the performance of the three modelling methods.

2.1 Data Collection and Processing

Data from seven perimeter offices in an academic building in Ottawa, Canada, are collected from November 2019 to January 2020 at 15-minute intervals. As illustrated in Fig. 2, the seven offices are served by two VAV terminal boxes VB_1 and VB_2 that receive supply air from an AHU. The supply air is reheated in the VBs and discharged into the offices via discharge air diffusers. These perimeter offices are provided with hydronic radiant heaters that use hot water from a steam/hot water heat exchanger. The radiant heaters are equipped with modulating valves to control the hot water flow rate into the offices. The seven offices are considered as seven thermal zones since each office uses an independent radiant heater to control the office temperature during the period of this study. The zone air temperature, $T_{z,1}(℃)$ to $T_{z,7}(℃)$, modulating valve state, $X_1(\%)$ to $X_7(\%)$, and the occupancy indicators, B_1 to B_7 , are measured

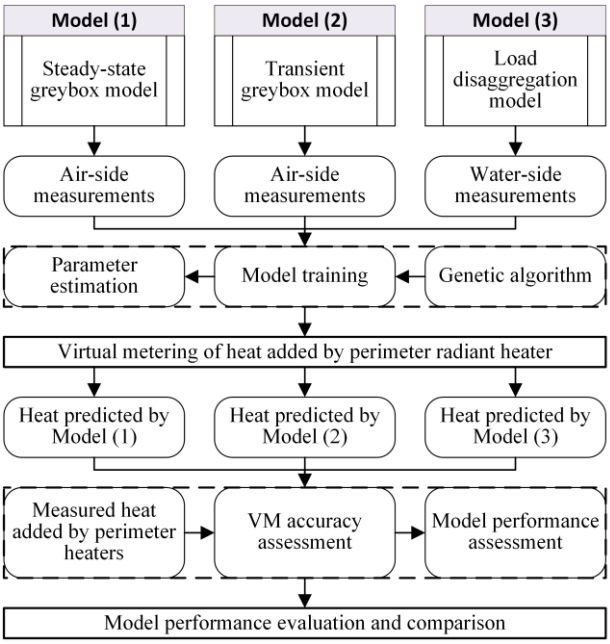

Figure 1: Schematic illustrating the use of three distinct modelling methods to develop zone-level radiant heater VMs. The accuracy of the VMs is used to evaluate the performance of the modelling methods

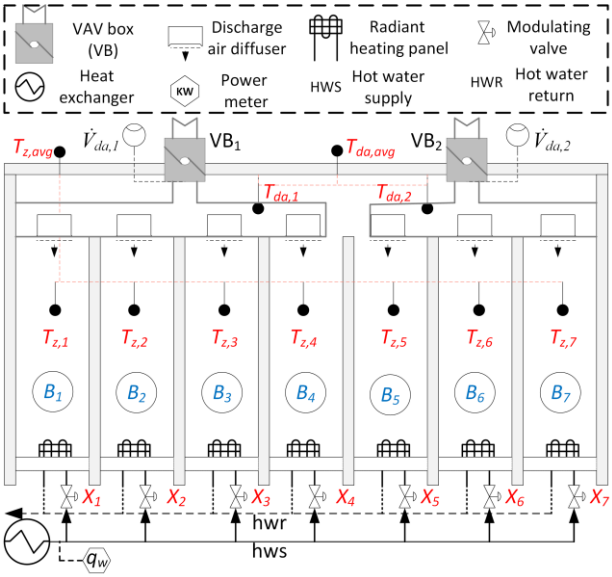

Figure 2: Data collected from seven perimeter zones in the academic building. $T_{z,i}$(℃), X_i(%), and B_i are zone air temperature, modulating valve state, and occupancy indicator in zone (i), respectively. $T_{da,j}$(℃) and $\dot{V}_{da,j}$(m^3/s) are the discharge air temperature and discharge airflow rate from VB_j, respectively. q_w(kW) represents the total hot water load.

at each zone, whereas the discharge air temperature, $T_{da,1}$(℃) and $T_{da,2}$(℃), and discharge airflow rate, $\dot{V}_{da,1}(m^3/s)$ and $\dot{V}_{da,2}(m^3/s)$, are measured at the two VAV terminal boxes. Additionally, the total hot water load, $q_w(kW)$, is measured at the heat exchanger hot water outlet. The zone air temperature and the discharge air temperature are modelled as single temperature nodes by averaging the measured data at every time step (Bleil et al., 2012; Platt et al., 2010). The total discharge airflow rate is obtained by summing up the discharge airflow rates from the two VAV terminal boxes VB_1 and VB_2. Finally, the binary occupancy signals (*i.e.,* 0 for non-occupied, 1 for occupied) are summed up for the seven zones. The processed dataset is used to train the three model structures developed in the following section.

2.2 Development of Zone Model Structures

Three distinct model structures are developed by applying a transient inverse greybox modelling method, a steady-state inverse greybox modelling method, and a load disaggregation modelling method. A description of each modelling method is provided in the following sections.

2.2.1 Transient inverse greybox modelling method

As shown in Fig. 3, the primary sources of heat gains and losses at a perimeter zone are internal heat gains from lights, occupants, and equipment, $q_{ig}(W)$, heat transfer through the envelope, $q_{env}(W)$, heat added or extracted through the discharge air diffuser, $q_{da}(W)$, solar heat gains, $q_{sol}(W)$, and heat added by the radiant panels, $q_{rad}(W)$. The rate of change in zone internal energy can be expressed as (Afram et al., 2014a; Nassif et al., 2008b):

$$c_a \cdot \rho_a \cdot V_z \cdot \frac{dT_z}{dt} = q_{da} + q_{env} + q_{rad} + q_{ig} + q_{sol} \quad (1)$$

where c_a is the specific heat of air (1000 $J/kg.℃$ at 20 ℃), ρ_a is the density of air (1.225 kg/m^3), T_z (℃) is the zone air temperature, and V_z (m^3) is the zone volume. The transient heat flow is approximated by an equivalent RC network with one resistance and one capacitance (*i.e.,* 1R1C network), as described in Fig. 4. The thermal capacitance, C_z (J/℃), represents the lumped thermal capacitance of a zone; and the thermal resistance, R_z (℃/W), represents the effective thermal resistance between zone indoors and outdoors, including heat transfer through the zone envelope and via air infiltration. Taking these terms into consideration, Equation (1) can be rewritten as (Gunay et al., 2016):

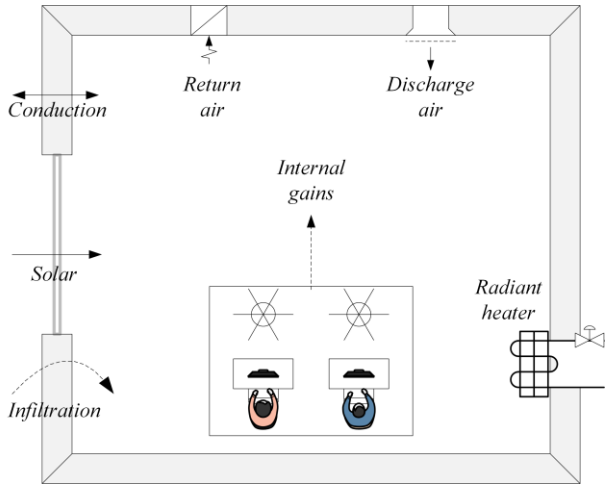

Figure 3: A schematic representation showing the primary sources of heat gains/losses in a single building VAV zone.

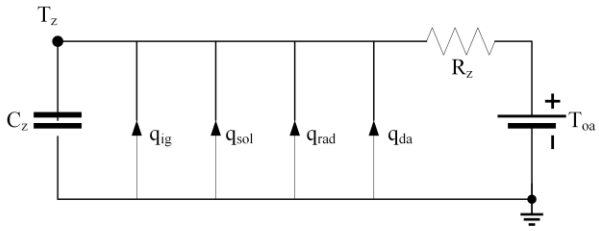

Figure 4: An approximation of transient heat flow with an equivalent thermal network comprising one resistance and one capacitance (*i.e.*, 1R1C network). Temperatures (℃) of zone air (T_z) and outdoor air (T_{oa}) are presented as electric voltages, whereas heat gains (W) from internal heat gains (q_{ig}), solar radiation (q_{sol}), radiant panels (q_{rad}), and discharge air (q_{da}) are presented as electric current. C_z ($J/$℃) and R_z (℃$/W$) represent the lumped thermal capacitance and resistance of the zone, respectively.

$$C_z \cdot \frac{dT_z}{dt} = \dot{V}_{da} \cdot c_a \cdot \rho_a \cdot (T_{da} - T_z) + \frac{(T_{oa} - T_z)}{R_z} + q_{rad} + q_{ig} + q_{sol} \quad (2)$$

where $\dot{V}_{da}$ (m^3/s) is the discharge airflow rate into the zone; and T_{da} (℃) and T_{oa} (℃) are the discharge air temperature and outdoor air temperature, respectively. A linear relationship is assumed between the hot water modulating valve state, X_{rad} (%), and the heat added by the radiant heater, q_{rad} (W), and between the binary occupancy indicator, B, and internal heat gains from lights, occupants, and equipment, q_{ig} (W). The impact of solar heat gains, q_{sol} (W), on the zone energy balance is minimized by only considering data points occurring after 4 pm and before 9 am. Under these assumptions, Equation (2) is further expanded to estimate the heat added or extracted through the discharge air diffuser as follows:

$$\dot{V}_{da} \cdot c_a \cdot \rho_a \cdot \left(T_z^{k-1} - T_{da}^{k-1}\right) = \frac{(T_{oa}^{k-1} - T_z^{k-1})}{x_1} + x_2 \cdot B^{k-1} + d \cdot X^{k-1} - x_3 \cdot \frac{T_z^k - T_z^{k-1}}{\Delta t} \quad (3)$$

where the superscript k is the index number of measured data, and Δt (s) is the time step interval. Parameters x_1 to x_3 estimate the effect of the zone thermal resistance, internal heat gains, and the transient response of zone thermal capacitance, respectively, on the energy balance of the zone, and parameter d estimates the capacity of the radiant heater. Equation (3) represents a single-zone model that can be expanded to multi-zones by taking the average zone air temperature, $T_{z,avg}$(℃), the average discharge air temperature, $T_{da,avg}$(℃), the total airflow rate from the discharge air diffusers, $\sum \dot{V}_{da,i}(m^3/s)$, and the total occupancy indicator from the individual zones, $\sum B_i$. Hence, the transient inverse greybox model for the seven perimeter zones is expressed as:

$$c_a \cdot \rho_a \cdot \sum_{i=1}^{7} \dot{V}_{da,i}^{k-1} \cdot \left(T_{z,avg}^{k-1} - T_{da,avg}^{k-1}\right) = \frac{\left(T_{oa}^{k-1} - T_{z,avg}^{k-1}\right)}{x_1} + x_2 \cdot \sum_{i=1}^{7} B_i^{k-1} + \left(\sum_{i=1}^{7} d_i \cdot X_i^{k-1}\right) - \left(x_3 \cdot \frac{T_{z,avg}^k - T_{z,avg}^{k-1}}{\Delta t}\right) + e \quad (4)$$

Parameters d_1 to d_7 estimate the capacity of the radiant heaters in Zones (1) to (7), and parameter e is an error term that accounts for unmodelled heat flows within the zone.

2.2.2 Steady-state inverse greybox modelling method

The steady-state modelling method assumes no thermal storage in the zone and hence no change in the zone air temperature occurs over time (Nassif et al., 2008b). The steady-state model is formulated by omitting the transient term in Equation (4) (*i.e.,* $T_{z,avg}^k - T_{z,avg}^{k-1} = 0$) as follows:

$$c_a \cdot \rho_a \cdot \left(\sum_{i=1}^{7} \dot{V}_{da,i}^{k-1}\right) \cdot \left(T_{z,avg}^{k-1} - T_{da,avg}^{k-1}\right) = \left(\frac{\left(T_{oa}^{k-1} - T_{z,avg}^{k-1}\right)}{x_1}\right) + \left(x_2 \cdot \sum_{i=1}^{7} B_i^{k-1}\right) + \left(\sum_{i=1}^{7} d_i \cdot X_i^{k-1}\right) + e \quad (5)$$

Since the steady-state modelling method neglects the transiency of the heat and mass transfer processes, the measured data can be averaged over more extended sampling periods (*i.e.*, downsampling). The impact of temporal averaging of data on the steady-state model's performance is evaluated by averaging the data collected from Zones (1) to (7) over sampling periods ranging from 0.25 hours to 24 hours. VMs results corresponding to each sampling period are compared with measured heat to assess the impact of temporal averaging of data on the accuracy of the VMs.

2.2.3 Load disaggregation modelling method

The load disaggregation method breaks down the total energy supplied to a group of radiant heaters into individual radiant heater energy components based on the state of the modulating valve. As illustrated in Fig. 5, hot water is provided by a steam/hot water heat exchanger that distributes hot water to the radiant heaters in the seven perimeter zones. The total hot water load, q_w (kW), is disaggregated across the seven radiant heaters by utilizing the modulating valve analog signals, X_i (%) , that control the hot water flow rate into the zone-level radiant heaters as expressed in Equation (6).

$$q_w = \left(\sum_{i=1}^{7} d_i \cdot X_i\right) + e \quad (6)$$

Model parameters d_1 to d_7 correspond to individual radiant heater capacities at Zones (1) to (7), respectively, and the error term e accounts for errors in the measured data and any potential leakage.

2.3 Virtual Metering and Model Performance Evaluation

The dataset created for the seven perimeter zones is used to train the three model structures given by Equations (4) to (6). An optimization problem is formulated to minimize the root-mean-square error (RMSE) between the estimated and measured discharge air load, q_{da} (kW), for the transient and steady-state models, and between estimated and measured total hot water load, q_w (kW), for the load disaggregation model. The GA is selected to solve the optimization problem and search for optimal model parameters since the upper and lower bounds for the parameters can be identified from the physical quantities presented by the models. The estimated values of model parameters

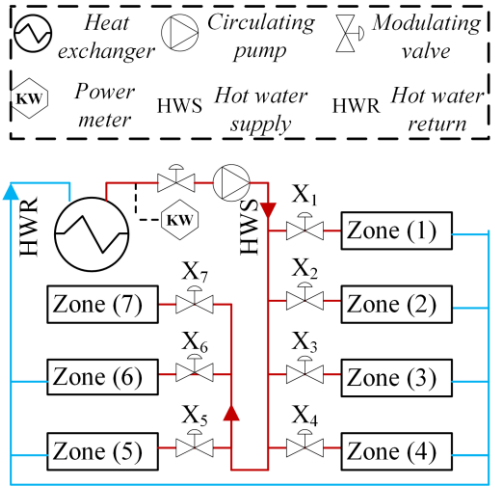

Figure 5: A schematic showing the disaggregation of total hot water load measured at the outlet of a steam/hot water heat exchanger across zone-level radiant heaters using the modulating valve state signals X_1 to X_7.

corresponding to each modelling method are used to create VMs to estimate the daily heat added by the radiant heaters, $\hat{E}_{rad,daily}$ (kWh/day), at each of the seven perimeter zones. The daily heat is obtained by summing the energy at 15-minute intervals for each zone as follows:

$$\hat{E}_{rad,daily} = \sum_{k=1}^{M} \hat{E}_{rad}^{k} = \sum_{k=1}^{M} (q_{rad}^{k} \cdot \Delta t) \tag{7}$$

where $\hat{E}_{rad}^{k}$ (kWh) is the estimated heat added during time step k, Δt (hrs) is the timestep interval, and M represents the number of time steps in one day. Measured data collected from physical meters are used to calculate the actual daily heat added by radiant heaters, $E_{rad,daily}$ (kWh/day) at Zones (1) to (7). The measured daily heat is utilized to verify the VM results using the RMSE (kWh/day) normalized by the range of daily measured heat at each zone (NRMSE), as follows:

$$NRMSE = \frac{\sqrt{\frac{1}{M} \cdot \sum_{k=1}^{M} (\hat{E}_{rad,daily}^{k} - E_{rad,daily}^{k})^2}}{(E_{rad,daily}^{max} - E_{rad,daily}^{min})} \tag{8}$$

where $E_{rad,daily}^{max}$ and $E_{rad,daily}^{min}$ represent the maximum and minimum values of measured daily heat. The accuracy of the VMs is used to analyze the performance of the steady-state, transient, and load disaggregation models. The three modelling methods are compared in terms of modelling assumptions, data requirements, and VMs accuracy.

3. RESULTS AND DISCUSSION

VM results corresponding to the three modelling methods are compared with measured heat collected from physical meters at Zones (1) to (7) to assess the accuracy of the VMs and evaluate the performance of the underlying modelling methods. As shown in Table 1, the three modelling methods can estimate the daily heat added by radiant heaters at an average NRMSE between 13% and 23%. The average RMSE from the seven zones for the transient modelling method, the steady-state modelling method, and the load disaggregation modelling method is $1.73\ kWh/day$, $2.67\ kWh/day$, and $1.63\ kWh/day$, respectively, as shown in Fig. 6. These results indicate better performance for the transient and load disaggregation modelling methods as compared to the steady-state modelling method. The decrease in accuracy for the VMs developed using a steady-state modelling method can be related to steady-state modelling assumptions and model inputs. For example, Fig. 7 shows the total estimated heat supplied by radiant heaters at Zones (1) to (7) from November 2019 to January 2020 using the three modelling methods. The total

Table 1: VM results assessment for the three modelling approaches

	Zone 1	**Zone 2**	**Zone 3**	**Zone 4**	**Zone 5**	**Zone 6**	**Zone 7**	**Overall**
Total measured heat (kWh)	334.61	231.05	274.83	405.67	335.29	194.02	357.63	2133.10
	Transient inverse greybox modelling approach							
Measured data required	$[T_{oa}(℃)]$, $[T_z(℃)]$, $[T_{da}(℃)]$, $[\dot{V}_z\ (m^3/s)]$, (B_z), $[X_z\ (\%)]$							
Total estimated heat (kWh)	346.23	216.06	337.19	460.02	357.57	177.06	359.34	2253.48
RMSE (kWh/day)	1.62	1.95	1.59	2.05	1.86	1.39	1.52	1.73
NRMSE (%)	19.29%	18.12%	23.19%	21.31%	15.36%	17.31%	13.04%	14.01%
	Steady-state inverse greybox modelling approach							
Measured data required	$[T_{oa}(℃)]$, $[T_z(℃)]$, $[T_{da}(℃)]$, $[\dot{V}_z\ (m^3/s)]$, (B_z), $[X_z\ (\%)]$							
Total estimated heat (kWh)	141.37	51.55	259.10	118.90	88.51	161.42	103.90	924.73
RMSE (kWh/day)	2.57	2.85	1.34	3.60	3.47	1.42	3.46	2.67
NRMSE (%)	30.66%	26.45%	19.52%	37.37%	28.62%	17.71%	29.65%	22.84%
	Load disaggregation modelling approach							
Measured data required	$[q_w\ (kW)]$, $[X_z\ (\%)]$							
Total estimated heat (kWh)	332.01	222.47	283.02	393.81	324.88	182.77	356.08	2095.03
RMSE (kWh/day)	1.58	1.95	1.36	1.74	1.82	1.39	1.52	1.63
NRMSE (%)	18.80%	18.10%	19.79%	18.09%	15.03%	17.26%	13.03%	13.26%

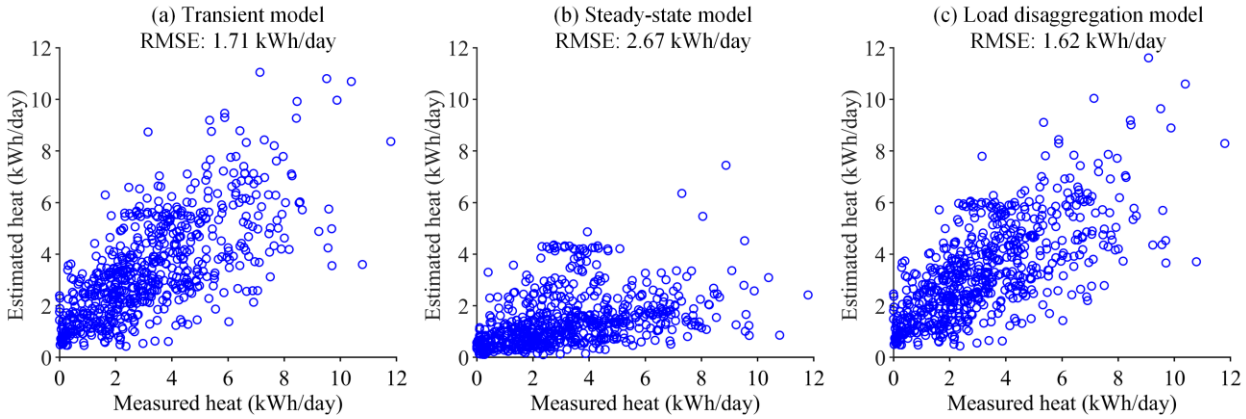

Figure 6: Predictive accuracy of VMs in the seven zones of the academic building developed by using (a) a transient modelling method, (b) a steady-state modelling method, and (c) a load disaggregation modelling method

Estimated heat for the seven zones when applying the steady-state modelling method is around 43% of the total measured heat. This substantial difference between the measured and estimated heat is believed to be related to the steady-state model structure, which assumes that no change in zone air temperature occurs over time. By checking the zone air temperature behaviour in Zone (3) for three days in January 2020, as shown in Fig. 8, it is noticed that the zone air temperature starts to decline when the VAV system shuts down at 22:45 hrs., and rises again upon VAV system start-up at 7:00 hrs. During the VAV system shut-down and start-up periods, the zone exhibits a dynamic behaviour not captured by the steady-state model. When data points corresponding to these periods are used as model inputs, the accuracy of the VMs declines, as indicated in Table 1.

The results presented in Table 1 are obtained using a 15-minute data sampling frequency for the three modelling methods. At this sampling frequency, a higher error is noticed for the steady-state modelling method than the transient and load disaggregation modelling methods (see Table 1). The impact of temporal averaging of measured

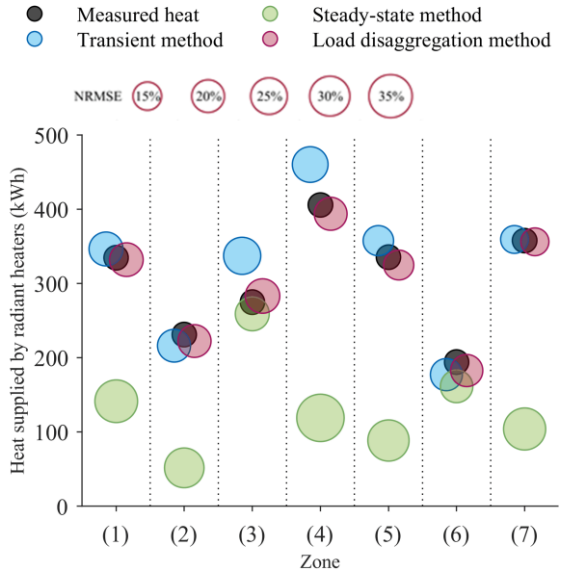

Figure 7: Estimated heat supplied by radiant heaters at Zones (1) to (7) from November 2019 to January 2020 using three modelling methods. The size of the bubble is proportional to the NRMSE obtained for each zone.

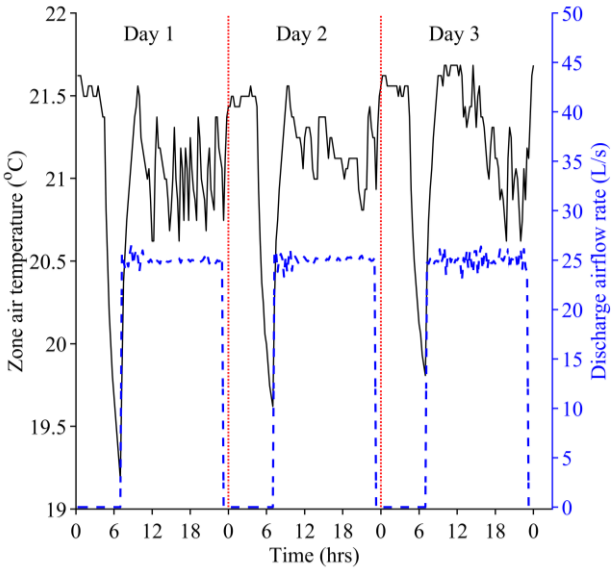

Figure 8: Zone air temperature in Zone (3) for three days in December 2019. During the start-up and shut-down of the VAV system, the zone's dynamic behaviour is not captured by the steady-state modelling method due to modelling assumptions.

data on the accuracy of the steady-state modelling method is examined by training the steady-state model using datasets averaged over sampling periods from 15 minutes to 24 hours. VMs are developed using the parameters identified from the trained models corresponding to each sampling period. As shown in Fig. 9, the average NRMSE of the VMs from the seven zones declines from 23% at a 15-minute sampling period to 13% when the sampling period is extended to 24 hours. The total predicted heat added by the radiant heaters in the seven zones compared to the measured heat indicates a better performance of the steady-state model at longer sampling periods. The decline in error at more extended sampling periods is attributed to minimizing the transient effect when the measured data is averaged over intervals with similar initial and final conditions. For example, the transient effect caused by starting-up and shutting-down the VAV system in Fig. 8 can be minimized by averaging the data over a 24-hour sampling period. Although using longer sampling periods with the steady-state modelling method improves the VM accuracy, additional data processing is required to average the data over longer sampling periods. In contrast, short sampling periods are appropriate for the transient and load disaggregation modelling methods.

Since the three modelling methods require different sorts of data, the availability of measured data from the BAS can be used as a means to select an appropriate modelling method. Measurements of outdoor air temperature, T_{oa}(℃), zone air temperature, $T_{z,i}$(℃), occupancy indicator, B_i, discharge airflow rate, $\dot{V}_{da,i}$, and radiant heater modulating valve position, X_i (%), are often available in the BAS of commercial and institutional buildings. However, measurements of discharge air temperature from the VAV system, $T_{da,i}$ (℃), and total hot water load from the steam/hot water heat exchanger, q_w (kW), are not always available. In cases when the total hot water load measurement is not available, the transient or the steady-state models should be selected, provided that the measurements required for these two modelling methods are available. Similarly, in cases when the measurement of discharge air temperature is not available, the load disaggregation modelling approach should be selected, provided that the total hot water load measurement is available. Hence, the availability of sensors and meters plays a critical role in the model selection process.

This study demonstrates the use of a steady-state modelling method, a transient modelling method, and a load disaggregation modelling method for creating VMs that estimate the heat added by zone-level perimeter heaters. The three modelling methods are compared in terms of modelling assumptions, data requirements, and virtual metering accuracy. The models developed upon applying these three modelling methods can be integrated into the BAS to estimate unmetered heat added by perimeter heaters. The estimated heating energy at a building zone-level provides critical information to building operators and facility managers to improve building energy performance and facilitate operational decisions.

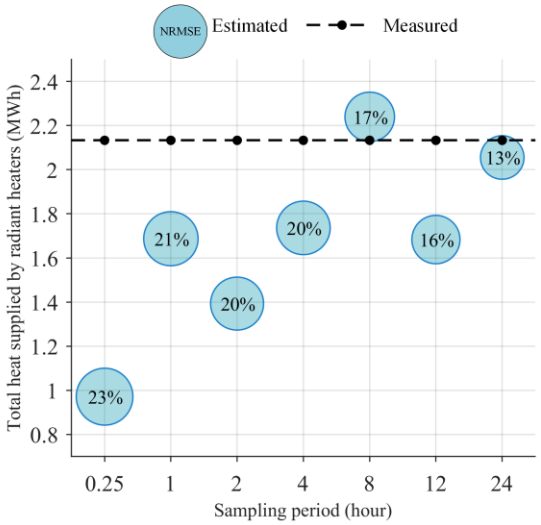

Figure 9: Total estimated heat supplied by the radiant heaters in Zones (1) to (7) compared to measured heat using the steady-state modelling method. Measurements are averaged over sampling periods from 15 minutes to 24 hours. The size of the bubble is proportional to the NRMSE obtained for each sampling period.

4. CONCLUSION

This paper evaluated the performance of three zone modelling methods used in developing VMs that can estimate the heat supplied by zone-level perimeter radiant heaters. Zone models were developed by applying a transient inverse greybox modelling method, a steady-state inverse greybox modelling method, and a load disaggregation modelling method. The models were trained using a dataset comprising three months of measured data collected from seven offices in an academic building in Ottawa, Canada. VMs were created by using model parameters that were identified using the genetic algorithm. The accuracy of the VMs was assessed using additional heat measurements collected from physical meters installed at the seven offices. The three modelling methods were compared in terms of modelling assumptions, model data requirements, and VMs accuracy.

The VMs' accuracy assessment showed that the three modelling methods could estimate the heat added by perimeter radiant heaters at an average NRMSE between 13% and 23%. The accuracy of the steady-state modelling method was further analyzed by checking the impact of temporal averaging of measured data over longer sampling periods. The results showed that the NRMSE improves by 10% when the sampling period increases from 15 minutes to 24 hours.

The model selection process was discussed by comparing the measurements required for the three modelling methods. Practical scenarios were presented, showing how the availability of measured data from the BAS impacts the selection of a suitable modelling method. Although an initial evaluation of the three modelling approaches was presented in this paper, there remain several unresolved issues for future research such as a) evaluating the performance of the three modelling methods as the number of zones increases, and b) developing visualization tools to present the VMs results to different building stakeholders.

ACKNOWLEDGEMENT

This research is supported by the research funding provided by the National Sciences and Engineering Research Council (NSERC) of Canada, Brookfield Global Integrated Solutions (BGIS), Public Services and Procurement Canada (PSPC), and CopperTree Analytics.

REFERENCES

Abushakra, B. (1999). An inverse model to predict and evaluate the energy performance of large commercial and institutional buildings. In *IBPSA Building Simulation* (Vol. 8, pp. 8–49). Retrieved from http://www.ibpsa.org/%5Cproceedings%5CBS1997%5CBS97_P183.pdf

Afram, A., & Janabi-Sharifi, F. (2014a). Review of modeling methods for HVAC systems. *Applied Thermal Engineering*. https://doi.org/10.1016/j.applthermaleng.2014.03.055

Afram, A., & Janabi-Sharifi, F. (2014b). Review of modeling methods for HVAC systems. *Applied Thermal Engineering*, *67*(1–2), 507–519. https://doi.org/10.1016/j.applthermaleng.2014.03.055

Albatici, R., Tonelli, A. M., & Chiogna, M. (2015). A comprehensive experimental approach for the validation of quantitative infrared thermography in the evaluation of building thermal transmittance. *Applied Energy*, *141*, 218–228. https://doi.org/10.1016/j.apenergy.2014.12.035

Bacher, P., & Madsen, H. (2011). Identifying suitable models for the heat dynamics of buildings. *Energy and Buildings*, *43*(7), 1511–1522. https://doi.org/10.1016/j.enbuild.2011.02.005

Balan, R., Cooper, J., Chao, K. M., Stan, S., & Donca, R. (2011). Parameter identification and model based predictive control of temperature inside a house. *Energy and Buildings*, *43*, 748–758. https://doi.org/10.1016/j.enbuild.2010.10.023

Bleil, C., Souza, D., & Alsaadani, S. (2012). Thermal zoning in speculative office buildings: discussing the connections between space layout and inside temperature control.

Braun, J. E., & Chaturvedi, N. (2002). An inverse gray-box model for transient building load prediction. *HVAC and R Research*, *8*(1), 73–99. https://doi.org/10.1080/10789669.2002.10391290

Candanedo, J. A., Dehkordi, V. R., & Lopez, P. (2013). A control-oriented simplified building modelling strategy. In *Proceedings of BS 2013: 13th Conference of the International Building Performance Simulation Association* (pp. 3682–3689).

Capozzoli, A., Lauro, F., & Khan, I. (2015). Fault detection analysis using data mining techniques for a cluster of smart office buildings. *Expert Systems with Applications*, *42*(9), 4324–4338. https://doi.org/10.1016/j.eswa.2015.01.010

Corrado, V., & Fabrizio, E. (2007). Assessment of building cooling energy need through a quasi-steady state model: Simplified correlation for gain-loss mismatch. *Energy and Buildings*, *39*(5), 569–579. https://doi.org/10.1016/j.enbuild.2006.09.012

Dall' o', G., Galante, A., & Torri, M. (2012). A methodology for the energy performance classification of residential building stock on an urban scale. *Energy and Buildings*, *48*, 211–219. https://doi.org/10.1016/j.enbuild.2012.01.034

Dinesh, C., Nettasinghe, B. W., Godaliyadda, R. I., Ekanayake, M. P. B., Ekanayake, J., & Wijayakulasooriya, J. V. (2016). Residential Appliance Identification Based on Spectral Information of Low Frequency Smart Meter Measurements. *IEEE Transactions on Smart Grid*, *7*(6), 2781–2792. https://doi.org/10.1109/TSG.2015.2484258

Dong, B., Cao, C., & Lee, S. E. (2005). Applying support vector machines to predict building energy consumption in tropical

region. *Energy and Buildings*, *37*(5), 545–553. https://doi.org/10.1016/j.enbuild.2004.09.009
Firth, S. K., & Lomas, K. J. (2009). INVESTIGATING CO 2 EMISSION REDUCTIONS IN EXISTING URBAN HOUSING USING A COMMUNITY DOMESTIC ENERGY MODEL. *Building Simulation*.
Gunay, B., Shen, W., & Newsham, G. (2017). Inverse blackbox modeling of the heating and cooling load in office buildings. *Energy and Buildings*, *142*, 200–210. https://doi.org/10.1016/j.enbuild.2017.02.064
Gunay, H. B., Bursill, J., Huchuk, B., O'Brien, W., & Beausoleil-Morrison, I. (2014). Shortest-prediction-horizon model-based predictive control for individual offices. *Building and Environment*, *82*, 408–419. https://doi.org/10.1016/j.buildenv.2014.09.011
Gunay, H. B., O'Brien, W., & Beausoleil-Morrison, I. (2016). Control-oriented inverse modeling of the thermal characteristics in an office. *Science and Technology for the Built Environment*, *22*(5), 586–605. https://doi.org/10.1080/23744731.2016.1175893
Heo, Y., Choudhary, R., & Augenbroe, G. A. (2012). Calibration of building energy models for retrofit analysis under uncertainty. *Energy and Buildings*, *47*, 550–560. https://doi.org/10.1016/j.enbuild.2011.12.029
Homod, R. Z. (2013). Review on the HVAC System Modeling Types and the Shortcomings of Their Application. *Journal of Energy*, *2013*. https://doi.org/10.1155/2013/768632
Larson, E., Froehlich, J., Campbell, T., Haggerty, C., Atlas, L., Fogarty, J., & Patel, S. N. (2012). Disaggregated water sensing from a single, pressure-based sensor: An extended analysis of HydroSense using staged experiments. *Pervasive and Mobile Computing*, *8*(1), 82–102. https://doi.org/10.1016/j.pmcj.2010.08.008
Ma, J., Qin, J., Salsbury, T., & Xu, P. (2012). Demand reduction in building energy systems based on economic model predictive control. *Chemical Engineering Science*, *67*(1), 92–100. https://doi.org/10.1016/j.ces.2011.07.052
Madsen, H. (2008). Time Series Analysis. 1st.
Madsen, Henrik, Bacher, P., Bauwens, G., Deconinck, A.-H., Reynders, G., Roels, S., … Lethé, G. (2016). Thermal Performance Characterization using Time Series Data. *IEA EBC Annex 58*.
Mayhorn, E. T., Sullivan, G. P., Butner, R. S., Hao, H., & Baechler, M. C. (2015). *Characteristics and Performance of Existing Load Disaggregation Technologies*. *Pacific Northwest National Laboratory, Richland, WS* (Vol. null). Richland, WA (United States). https://doi.org/10.2172/1203912
Nardi, I., Ambrosini, D., De Rubeis, T., Sfarra, S., Perilli, S., & Pasqualoni, G. (2015). A comparison between thermographic and flow-meter methods for the evaluation of thermal transmittance of different wall constructions. *Journal of Physics: Conference Series*, *655*(1). https://doi.org/10.1088/1742-6596/655/1/012007
Nassif, N., Moujaes, S., & Zaheeruddin, M. (2008a). Self-tuning dynamic models of HVAC system components. *Energy and Buildings*, *40*(9), 1709–1720. https://doi.org/10.1016/j.enbuild.2008.02.026
Nassif, N., Moujaes, S., & Zaheeruddin, M. (2008b). Self-tuning dynamic models of HVAC system components. *Energy and Buildings*, *40*(9), 1709–1720. https://doi.org/10.1016/J.ENBUILD.2008.02.026
Patri, O. P., Panangadan, A. V., Chelmis, C., & Prasanna, V. K. (2014). Extracting discriminative features for event-based electricity disaggregation. In *2014 IEEE Conference on Technologies for Sustainability, SusTech 2014* (pp. 232–238). Institute of Electrical and Electronics Engineers Inc. https://doi.org/10.1109/SusTech.2014.7046249
Platt, G., Li, J., Li, R., Poulton, G., James, G., & Wall, J. (2010). Adaptive HVAC zone modeling for sustainable buildings. *Energy and Buildings*, *42*(4), 412–421. https://doi.org/10.1016/j.enbuild.2009.10.009
Rabl, A. (1988). Parameter estimation in buildings: Methods for dynamic analysis of measured energy use. *Journal of Solar Energy Engineering, Transactions of the ASME*, *110*(1), 52–66. https://doi.org/10.1115/1.3268237
Ranade, A., Provan, G., El-Din Mady, A., & O'Sullivan, D. (2020). A computationally efficient method for fault diagnosis of fan-coil unit terminals in building Heating Ventilation and Air Conditioning systems. *Journal of Building Engineering*, *27*, 100955. https://doi.org/10.1016/j.jobe.2019.100955
Shi, Z., O'Brien, W., & Gunay, B. (2016). Building Zone Fault Detection with Kalmnan Filter based Methods. In *eSim 2016*. Retrieved from https://www.researchgate.net/publication/306006612
Široký, J., Oldewurtel, F., Cigler, J., & Prívara, S. (2011). Experimental analysis of model predictive control for an energy efficient building heating system. *Applied Energy*, *88*(9), 3079–3087. https://doi.org/10.1016/j.apenergy.2011.03.009
Thavlov, A. ;, & Bindner, H. W. (2012). *Thermal Models for Intelligent Heating of Buildings*. APA.
Valovage, M., & Gini, M. (2017). Label correction and event detection for electricity disaggregation. In *Proceedings of the International Joint Conference on Autonomous Agents and Multiagent Systems, AAMAS* (Vol. 2, pp. 990–998). Retrieved from www.ifaamas.org
Wang, B., Chen, Z., Boedihardjo, A. P., & Lu, C. T. (2018). Virtual metering: An efficient water disaggregation algorithm via non-intrusive load monitoring. *ACM Transactions on Intelligent Systems and Technology*, *9*(4), 1–30. https://doi.org/10.1145/3141770
Wang, H., Xu, P., Lu, X., & Yuan, D. (2016). Methodology of comprehensive building energy performance diagnosis for large commercial buildings at multiple levels. *Applied Energy*, *169*, 14–27. https://doi.org/10.1016/j.apenergy.2016.01.054
Yan, C., Wang, S., & Xiao, F. (2012). A simplified energy performance assessment method for existing buildings based on energy bill disaggregation. *Energy and Buildings*, *55*, 563–574. https://doi.org/10.1016/j.enbuild.2012.09.043
Zheng, K., Cho, Y. K., Wang, C., & Li, H. (2016). Noninvasive Residential Building Envelope R-Value Measurement Method Based on Interfacial Thermal Resistance. *Journal of Architectural Engineering*, *22*(4). https://doi.org/10.1061/(ASCE)AE.1943-5568.0000182